Volume 12
Number 12
December 2021
Pages 1979–2074

RSC Medicinal Chemistry

rsc.li/medchem

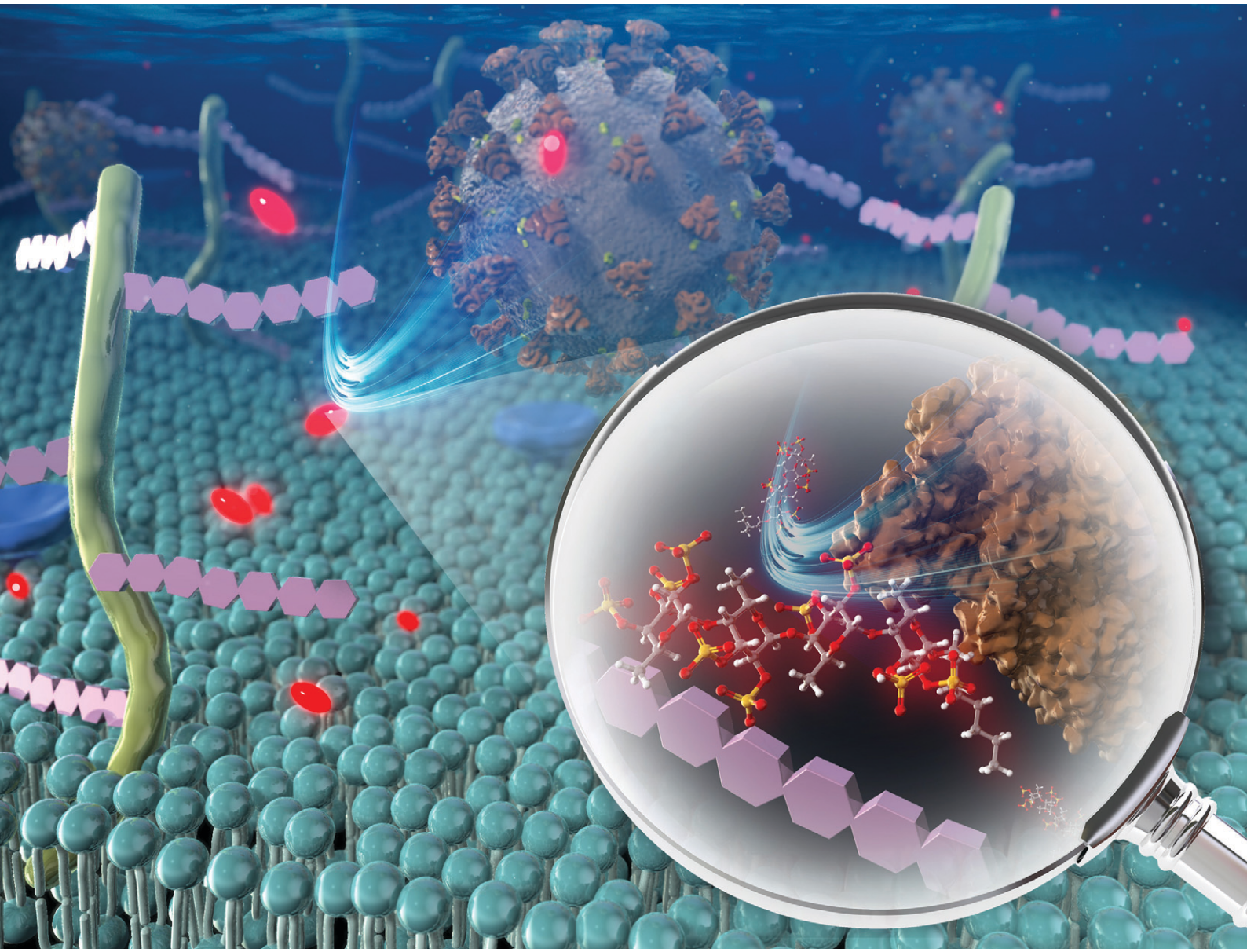

ISSN 2632-8682

ROYAL SOCIETY OF CHEMISTRY

RESEARCH ARTICLE
Daisuke Takahashi, Kazunobu Toshima *et al.*
Synthesis of low-molecular weight fucoidan derivatives and their binding abilities to SARS-CoV-2 spike proteins

RSC Medicinal Chemistry

ROYAL SOCIETY OF CHEMISTRY

RESEARCH ARTICLE

Cite this: *RSC Med. Chem.*, 2021, **12**, 2016

Synthesis of low-molecular weight fucoidan derivatives and their binding abilities to SARS-CoV-2 spike proteins†

Tatsuki Koike,[a] Aoi Sugimoto,[a] Shuhei Kosono,[a] Sumika Komaba,[a] Yuko Kanno,[a] Takashi Kitamura,[a] Itsuki Anzai,[b] Tokiko Watanabe,[b] Daisuke Takahashi *[a] and Kazunobu Toshima *[a]

Received 7th August 2021,
Accepted 6th September 2021

DOI: 10.1039/d1md00264c

rsc.li/medchem

Fucoidan derivatives **10**–**13**, whose basic sugar chains are composed of repeating α(1,4)-linked L-fucopyranosyl residues with different sulfation patterns, were designed and systematically synthesized. A structure–activity relationship (SAR) study examined competitive inhibition by thirteen fucoidan derivatives against heparin binding to the SARS-CoV-2 spike (S) protein. The results showed for the first time that **10** exhibited the highest inhibitory activity of the fucoidan derivatives used. The inhibitory activity of **10** was much higher than that of fondaparinux, the reported ligand of SARS-CoV-2 S protein. Furthermore, **10** exhibited inhibitory activities against the binding of heparin with several mutant SARS-CoV-2 S proteins, but was found to not inhibit factor Xa (FXa) activity that could otherwise lead to undesirable anticoagulant activity.

Introduction

The coronavirus disease 2019 (COVID-19) pandemic, caused by severe acute respiratory syndrome-related coronavirus 2 (SARS-CoV-2), is evolving rapidly worldwide and changing economic and public health conditions. To date, it has infected over 110 million people and caused more than 2.5 million deaths globally,[1] prompting rapid vaccine development and distribution and drug discovery research. Various drug candidates in development include agents to interfere with virus attachment to host cells.[2] Previous studies suggest that when SARS-CoV-2 enters host cells, SARS-CoV-2 spike (S) protein, consisting of S1 and S2 subunits, interacts with heparan sulfate (HS) on the cell surface through the S1/S2 proteolytic cleavage site. The receptor-binding domain (RBD) in the S1 subunit and/or S2 subunit then facilitates binding to the high affinity receptor angiotensin-converting enzyme 2 (ACE-2) to infect host cells effectively.[2,3] Some fucoidans (sulfated polysaccharides derived from seaweed and sea urchin) can reportedly bind to the SARS-CoV-2 S protein and effectively inhibit virus infection.[4] Fucoidan is thus a potential anti-SARS-CoV-2 agent, and elucidation of the detailed structure–activity relationship (SAR) for its binding to the SARS-CoV-2 S protein has attracted much attention.[5] In general, fucoidans can be classified into the three groups shown in Fig. 1.[6] One group (type I) includes the fucoidans isolated from, for example, *Cladosiphon okamuranus* and *Chorda filum*, whose basic sugar chains are composed of repeating α(1,3)-linked L-fucopyranosyl residues. The second group (type II) includes fucoidans isolated from, for example, *Ascophyllum nodosum* and *Fucus vesiculosus*, whose basic sugar chains are composed of repeating α(1,3)- and α(1,4)-linked

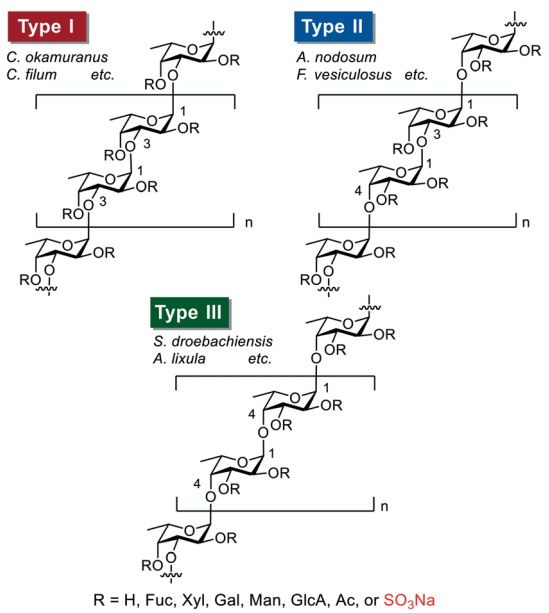

Fig. 1 Three types (I–III) of homofucose chains in fucoidans.

[a] *Department of Applied Chemistry, Faculty of Science and Technology, Keio University, 3-14-1 Hiyoshi, Kohoku-ku, Yokohama 223-8522, Japan. E-mail: dtak@applc.keio.ac.jp, toshima@applc.keio.ac.jp*
[b] *Department of Molecular Virology, Research Institute for Microbial Diseases, Osaka University, 3-1 Yamadaoka, Suita, Osaka 565-0871, Japan*

† Electronic supplementary information (ESI) available. See DOI: 10.1039/d1md00264c

L-fucopyranosyl residues. The third group (type III) includes the fucoidans isolated from, for example, *Strongylocentrotus droebachiensis* and *Arbacia lixula*, whose basic sugar chains are composed of repeating α(1,4)-linked L-fucopyranosyl residues. However, the structural heterogeneity and ununiformity of the sulfation patterns of naturally occurring fucoidans makes it difficult to conduct detailed SAR studies. We recently systematically synthesized type I and II fucoidan derivatives **1–9** with different sulfation patterns (Fig. 2) and evaluated their apoptosis-inducing activities against human cancer cells and their binding ability to influenza virus hemagglutinin (HA). The results showed that fucoidan derivative **7** possesses apoptosis-inducing activity against breast cancer MCF-7 and cervical epithelioid carcinoma HeLa cells.[7] In addition, fucoidan derivative **5** binds to influenza virus HA at the same binding site as the native sialoside ligand, inhibiting influenza virus infection.[8] In this context, here we designed and synthesized type III fucoidan derivatives with different sulfation patterns. In addition, we conducted a SAR study of competitive inhibition using thirteen fucoidan derivatives against heparin binding to the SARS-CoV-2 S protein.

Results and discussion

Synthesis of type III fucoidan derivatives 10–13

The designed type III fucoidan derivatives **10–13** with different sulfation patterns (2,3-*O*-sulfated type **10**, 3-*O*-sulfated type **11**, 2-*O*-sulfated type **12** and non-sulfated type **13**) are shown in Fig. 2. As shown in Scheme 1, we planned to synthesize **10–13** utilizing common key intermediate **16** with three types of protecting groups (benzyl (Bn), benzoyl (Bz) and *p*-methoxybenzyl (PMB)) at appropriate positions. Inititially we synthesized **16**. Thioglycoside **17** and trichloacetimidate **18** were prepared from L-fucose in 8 and 11 steps, respectively. Chemoselective glycosylation of **17** and **18** using $Yb(OTf)_3$ as an activator at −60 °C gave **19** with complete α-stereoselectivity. Hydrolysis of **19** using NIS/$Sc(OTf)_3$, followed by trichloroacetimidate formation, provided disaccharide donor **21**. Coupling reaction of **21** and 1-octanol using $Yb(OTf)_3$ at −60 °C proceeded to give **22** with complete β-stereoselectivity. Deprotection of the Bz group on **22** afforded disaccharide acceptor **23** in high yield. Next, we examined the glycosylation of **21** and **23** using TMSOTf in Et_2O at −80 °C. The reaction proceeded smoothly to provide the desired key intermediate **16** in 79% yield as a single isomer. We next synthesized the designed type III fucoidan derivatives **10–13** from **16**. Deprotection of the Bn and PMB groups on **16** under hydrogenolysis conditions, followed by methanolysis, provided the non-sulfated fucoidan derivative **13**. Sulfation of **13** using $SO_3{\cdot}NEt_3$ complex in DMF gave all-sulfated **10**. Alternatively, selective deprotection of the PMB groups on **16** using DDQ, followed by acetylation, hydrogenolysis, sulfation using the $SO_3{\cdot}NEt_3$ complex in DMF and saponification, provided 2-*O*-sulfated tetrasaccharide **12**. Deprotection of the PMB groups on **16**, followed by methanolysis, sulfation, and hydrogenolysis, afforded the desired 3-*O*-sulfated tetrafucoside **11**.

Binding affinity of heparin to SARS-CoV-2 S protein

With the thirteen designed fucoidan derivatives in hand, we used bio-layer interferometry (BLI) to study the binding of the fucoidan derivatives to wild type SARS-CoV-2 S protein

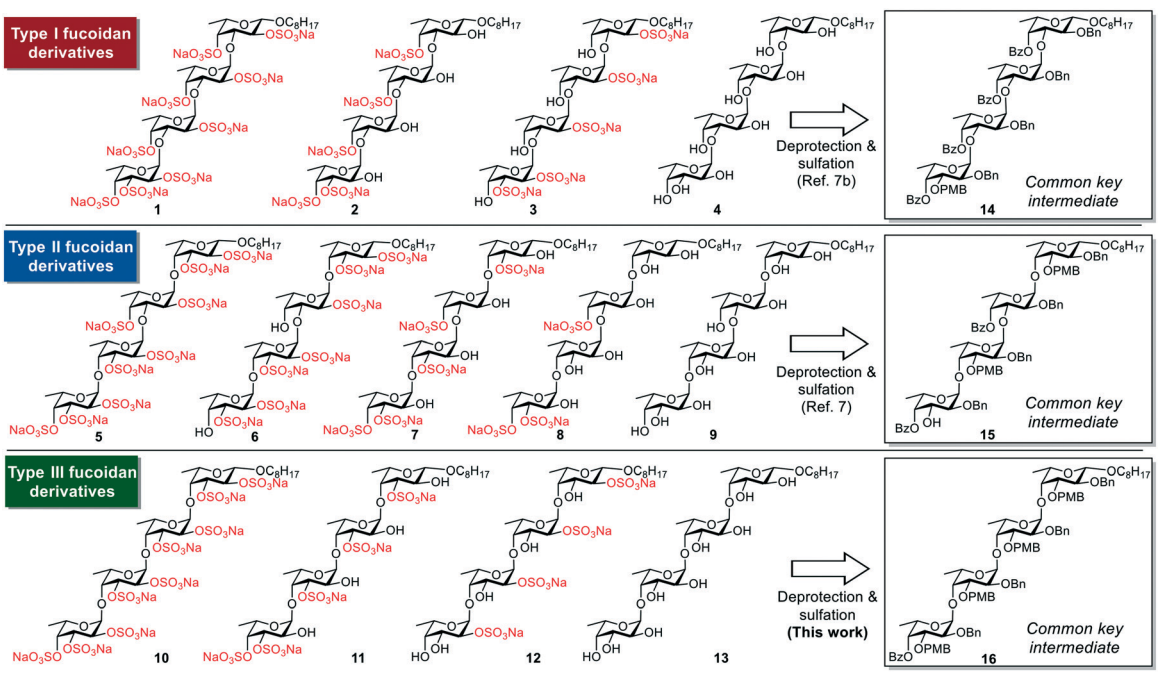

Fig. 2 Chemical structures of the fucoidan derivatives **1–13** and the common key intermediates **14–16**.

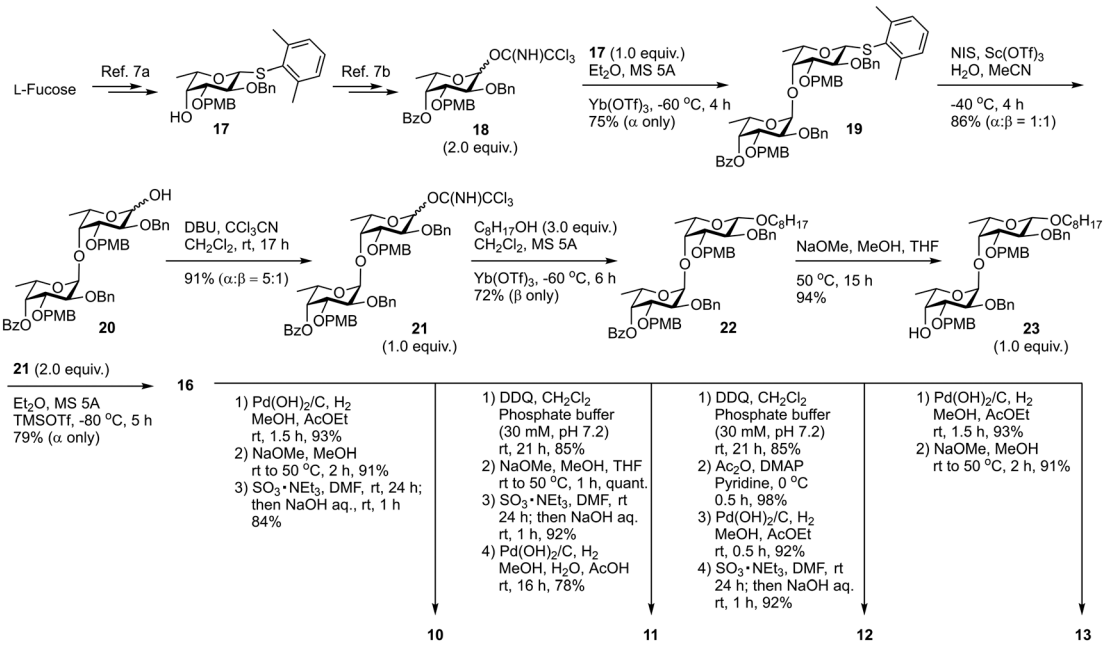

Scheme 1 Synthetic scheme for **16** and type III fucoidan derivatives **10**–**13**. PMB = *p*-methoxybenzyl; Et = ethyl; Me = methyl; Bn = benzyl; Bz = benzoyl; Tf = trifluoromethanesulfonyl; NIS = *N*-iodosuccinimide; MS = molecular sieves; DBU = 1,8-diazabicyclo[5,4,0]undec-7-ene; THF = tetrahydrofuran; TMS = trimethylsilyl; DDQ = 2,3-dichloro-5,6-dicyano-*p*-benzoquinone; Ac = acetyl; DMF = *N*,*N*-dimethylformamide; DMAP = 4-dimethylaminopyridine.

(S1 and S2). First, the BLI sensor tips functionalized with streptavidin were modified with different concentrations (0, 22.7, 45.5, 90.9, and 181.8 nM) of heparin–biotin. Next, each sensor chip was treated with 1 μM SARS-CoV-2 S protein (S1 and S2) in TBS (20 mM Tris, pH 7.4, containing 0.02% BSA) for 5 min. The corresponding BLI spectra for real-time monitoring of binding between heparin and SARS-CoV-2 S protein are shown in Fig. 3a. The BLI response signal increased in a concentration-dependent manner, and the dissociation constant (K_d) was calculated using the 1 : 1 Langmuir model to be 36.0 nM (Fig. 3b and c), in good agreement with reported data.[2b]

SAR study using 1–13 for competitive inhibition against heparin binding to SARS-CoV-2 S protein

Next, to measure the inhibitory activities of fucoidan derivatives **1**–**13** for the binding between SARS-CoV-2 S protein and heparin, BLI biosensors with immobilized heparin were dipped into a solution of SARS-CoV-2 S protein (1 μM) and each fucoidan derivative **1**–**13** (50 μM) in TBS. The FDA-approved heparin drug fondaparinux (**24**)[9] (Fig. 4a), a known binder[3c] to SARS-CoV-2 S protein, was used as a control. The results are shown in Fig. 4. All-sulfated type **10**, with a type III sugar backbone chain, exhibited the highest inhibitory activity, followed by all-sulfated type **5** with a type II sugar backbone chain. Non-sulfated type **4**, **9**, and **13** showed almost no inhibitory activity. Interestingly, all-sulfated type **1** with a type I sugar backbone chain exhibited low inhibitory activity (less than 10%). These results clearly indicate that slight differences in the sugar backbone chain and in the pattern of sulfate groups in **1** to **13** significantly affect inhibitory activity.

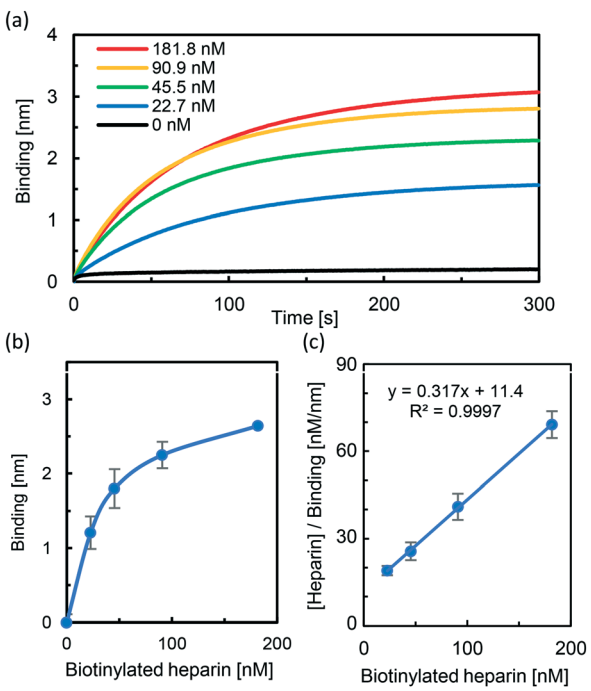

Fig. 3 Partial BLI sensor-grams for measuring the binding affinities of SARS-CoV-2 S protein to heparin. (a) Biotinylated heparin (0–181.8 nM) was immobilized to streptavidin biosensors which were then exposed to SARS-CoV-2 S protein (1 μM). (b) Plot of the BLI signal of the heparin-dose response of the binding affinity of SARS-CoV-2 S protein. (c) Binding kinetics was analyzed by fitting the 1 : 1 Langmuir model to evaluate the dissociation constant (K_d).

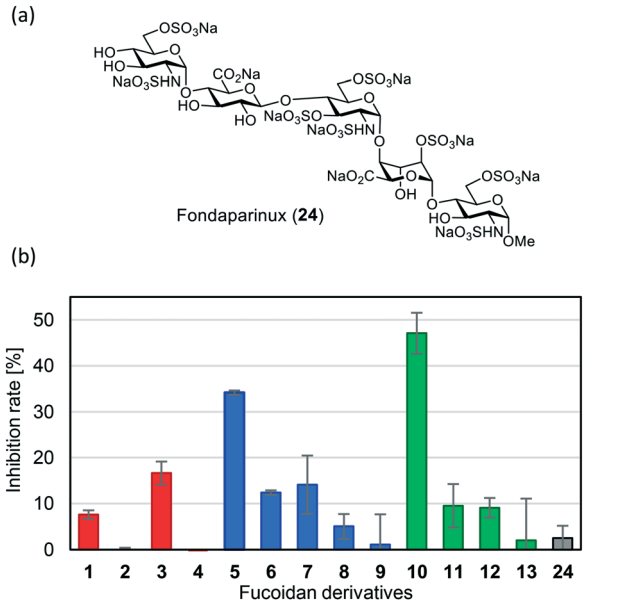

Fig. 4 (a) Chemical structure of fondaparinux (**24**). (b) Inhibitory activities of fucoidan derivatives **1**–**13** and **24** for binding between SARS-CoV-2 S protein and heparin. BLI biosensors with immobilized heparin were dipped into a solution of SARS-CoV-2 S protein (1 μM) and each fucoidan derivative **1**–**13** and **24** (50 μM) in 0.02% BSA/TBS. Inhibition rate (%) was determined by the decrease in the BLI signal.

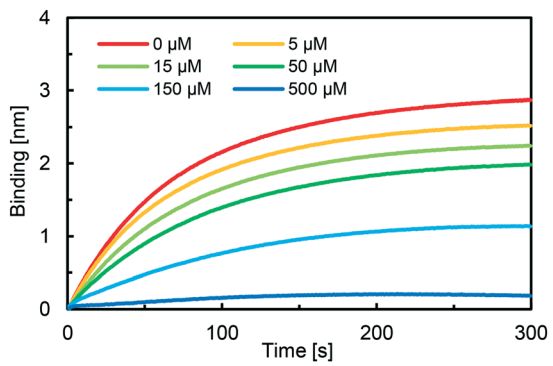

Fig. 5 Partial BLI sensor-grams of the competition assay between **10** and heparin. Biosensors with immobilized heparin were dipped into a solution containing SARS-CoV-2 S protein (1 μM) and **10** (0–500 μM). IC_{50} was evaluated by the inhibition rate using GraphPad Prism.

Furthermore, the inhibitory activity of **10** was much higher than that of **24**.

Binding affinity of 10 to several SARS-CoV-2 S proteins

Next, we measured the binding affinity of **10** to SARS-CoV-2 S protein using a competition assay. As shown in Fig. 5, the BLI signal decreased in a dose-dependent manner when the biosensor with immobilized heparin was incubated with a solution of SARS-CoV-2 S protein (1 μM) and different concentrations of **10** (0–500 μM). The IC_{50} value was calculated by nonlinear regression analysis using GraphPad Prism software to be 86.9 μM. In addition, the K_i value was calculated to be 3.02 μM using the Cheng–Prusoff equation,[10] indicating high affinity of compound **10** to SARS-CoV-2 S protein. Next, to show the generality and efficiency of compound **10**, the binding affinities of **10** to mutated SARS-CoV-2 S proteins derived from variants of concern (B.1.1.7, B.1.351, and P.1)[11] were evaluated by the same competition assay. It was found that **10** effectively bound to the three mutant SARS-CoV-2 S proteins in a dose dependent manner. The IC_{50} values were 35.0 μM, 85.9 μM and 65.6 μM for B.1.1.7, B.1.351, and P.1, respectively, as shown in Fig. 6, and the K_i values were calculated to be 10.1 μM, 6.67 μM and 6.98 μM, respectively. These results indicate that **10** can effectively inhibit the binding process between mutant SARS-CoV-2 S proteins and surface heparin.

Anti-factor Xa activities of 10 and 24

Anti-coagulant activity is a possible and serious side effect of the use of heparin drugs, including **24**, because these drugs can bind to antithrombin (AT III) and inactivate factor Xa (FXa), which leads to blood clot formation by converting prothrombin to thrombin through the prothrombinase complex.[12] Thus, to show the efficacy of fucoidan derivative **10**, the enzyme inhibitiory activity of **10** against FXa was examined using a Fxa-specific chromogenic substrate in Tris-EDTA buffer (50 mM Tris, 175 mM NaCl, 7.5 mM EDTA, 0.1% PEG, 0.9 g L^{-1} NaN_3, pH 8.4). The results are summarized in Fig. 7. When **24** was used as a control compound, significant inhibitory activity was

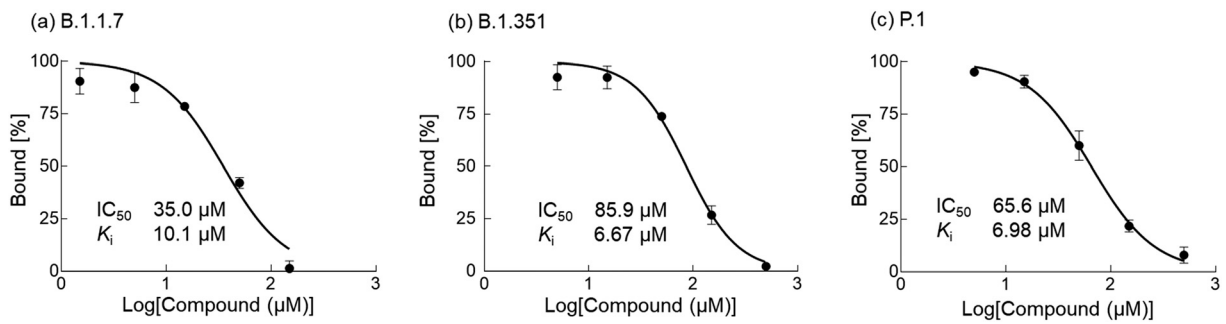

Fig. 6 Binding affinities of **10** to the mutant SARS-CoV-2 S proteins (B.1.1.7, B.1.351 and P.1). BLI biosensors with immobilized heparin were dipped into a solution of **10** (1.5–500 μM) and each mutant SARS-CoV-2 S protein (1 μM) in 0.02% BSA/TBS. Bound (%) was determined by the response of the BLI signal. IC_{50} values were calculated using GraphPad Prism software. K_i values of **10** to the mutant SARS-CoV-2 S proteins were calculated based on the IC_{50} values according to the Cheng–Prusoff equation.

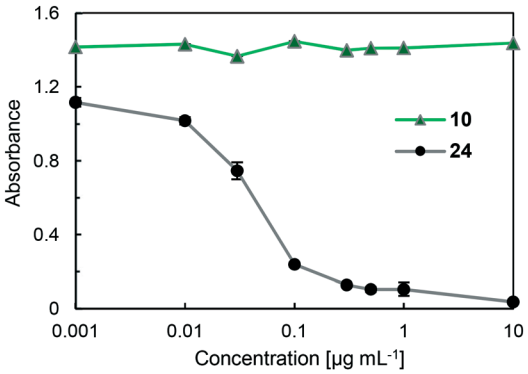

Fig. 7 Anti-FXa activities of **10** and fondaparinux (**24**) (0.001–10 μg mL^{-1}) in the presence of ATIII using an FXa specific chromogenic substrate in Tris-EDTA buffer. The absorbance was measured at 405 nm on a plate reader. The results are expressed as means ± the standard deviation (n = 3).

observed in a concentration-dependent manner. In sharp contrast, when compound **10** was used under the same conditions, no inhibitory activity against FXa was observed even at a high concentration (10 μg mL^{-1}), indicating that compound **10** is a promising candidate as an effective SARS-CoV-2 entry inhibitor targeting SARS-CoV-2 S protein.

Conclusions

In conclusion, purpose-designed fucoidan derivatives **10–13** possessing a type III sugar backbone chain with different sulfation patterns were systematically synthesized. A SAR study of competitive inhibition by fucoidan derivatives **1–13** against heparin binding to the SARS-CoV-2 S protein showed for the first time that **10** exhibited the highest inhibitory activity of the compounds synthesized, and the inhibitory activity of **10** was much higher than that of the known binder fondaparinux (**24**). Furthermore, **10** exhibited significant inhibitory activities for binding not only between heparin and wild type SARS-CoV-2 S protein, but also the three mutant SARS-CoV-2 S proteins of the variants of concern B.1.1.7, B.1.351 and P.1. Moreover, **10** did not inhibit FXa activity that could lead to undesirable anticoagulant activity. These results are expected to contribute to the development of effective new SARS-CoV-2 entry inhibitors targeting SARS-CoV-2 S protein.

Author contributions

DT and KT conceived and directed the project. TK, AS, SK, SK and YK performed the chemical syntheses. TK, AS and TK performed the binding experiments. IA and TW prepared the mutant SARS-CoV-2 S proteins. The first draft of this manuscript was prepared by TK and DT, and the final draft was edited by all the authors.

Conflicts of interest

There are no conflicts to declare.

Acknowledgements

This research was supported in part by JSPS KAKENHI Grant Number JP19H02724 in Scientific Research (B), JST CREST Grant Number JPMJCR20R3, and Keio Gijuku Academic Development Funds.

Notes and references

1 World Health Organization, Coronavirus disease (COVID-19) situation reports, WHO, https://www.who.int/emergencies/diseases/novel-coronavirus-2019/situation-reports (2021).

2 (*a*) D. S. Dimitrov, *Nat. Rev. Microbiol.*, 2004, **2**, 109; (*b*) L. Liu, P. Chopra, X. Li, K. M. Bouwman, S. M. Tompkins, M. A. Wolfert, R. P. de Vries and G.-J. Boons, *ACS Cent. Sci.*, 2021, **7**, 1009; (*c*) B. Hu, H. Guo, P. Zhou and Z. Shi, *Nat. Rev. Microbiol.*, 2021, **19**, 141.

3 (*a*) S. Y. Kim, W. Jin, A. Sood, D. W. Montgomery, O. C. Grant, M. M. Fuster, L. Fu, J. S. Dordick, R. J. Woods, F. Zhang and R. J. Linhardt, *Antiviral Res.*, 2020, **181**, 104873; (*b*) T. M. Clausen, D. R. Sandoval, C. B. Spliid, J. Pihl, H. R. Perrett, C. D. Painter, A. Narayanan, S. A. Majowicz, E. M. Kwong, R. N. McVicar, B. E. Thacker, C. A. Glass, Z. Yang, J. L. Torres, G. J. Golden, P. L. Bartels, R. N. Porell, A. F. Garretson, L. Laubach, J. Feldman, X. Yin, Y. Pu, B. M. Hauser, T. M. Caradonna, B. P. Kellman, C. Martino, P. L. M. S. Gordts, S. K. Chanda, A. G. Schmidt, K. Godula, S. L. Leibel, J. Jose, K. D. Corbett, A. B. Ward, A. F. Carlin and J. D. Esko, *Cell*, 2020, **183**, 1043; (*c*) W. Hao, B. Ma, Z. Li, X. Wang, X. Gao, Y. Li, B. Qin, S. Shang, S. Cui and Z. Tan, *Sci. Bull.*, 2021, **66**, 1205.

4 (*a*) P. S. Kwon, H. Oh, S.-J. Kwon, W. Jin, F. Zhang, K. Fraser, J. J. Hong, R. J. Linhardt and J. S. Dordick, *Cell Discovery*, 2020, **6**, 50; (*b*) R. Tandon, J. S. Sharp, F. Zhang, V. H. Pomin, N. M. Ashpole, D. Mitra, M. G. McCandless, W. Jin, H. Liu, P. Sharma and R. J. Linhardt, *J. Virol.*, 2021, **95**, e01987.

5 W. Jin, W. Zhang, D. Mitra, M. G. McCandless, P. Sharma, R. Tandon, F. Zhang and R. J. Linhardt, *Int. J. Biol. Macromol.*, 2020, **163**, 1649.

6 (*a*) A. Cumashi, N. A. Ushakova, M. E. Preobrazhenskaya, A. D'Incecco, A. Piccoli, L. Totani, N. Tinari, G. E. Morozevich, A. E. Berman, M. I. Bilan, A. I. Usov, N. E. Ustyuzhanina, A. A. Grachev, C. J. Sanderson, M. Kelly, G. A. Rabinovich, S. Iacobelli and N. E. Nifantiev, *Glycobiology*, 2007, **17**, 541; (*b*) V. H. Pomin and P. A. S. Mouraõ, *Glycobiology*, 2008, **18**, 1016.

7 (*a*) S. Arafuka, N. Koshiba, D. Takahashi and K. Toshima, *Chem. Commun.*, 2014, **50**, 9831; (*b*) A. Kasai, S. Arafuka, N. Koshiba, D. Takahashi and K. Toshima, *Org. Biomol. Chem.*, 2015, **13**, 10556.

8 S. Kosono, A. Kasai, S. Komaba, T. Matsubara, T. Sato, D. Takahashi and K. Toshima, *Chem. Commun.*, 2018, **54**, 7467.

9 K. A. Bauer, D. W. Hawkins, P. C. Peters, M. Petitou, J. M. Herbert, C. A. A. van Boeckel and D. G. Meuleman, *Cardiovasc. Drug Rev.*, 2002, **20**, 37.

10 Y. Cheng and W. H. Prusoff, *Biochem. Pharmacol.*, 1973, **22**, 3099.
11 W. T. Harvey, A. M. Carabelli, B. Jackson, R. K. Gupta, E. C. Thomson, E. M. Harrison, C. Ludden, R. Reeve, A. Rambaut, COVID-19 Genomiccs UK (COG-UK) Consortium, S. J. Peacock and D. L. Rovertson, *Nat. Rev. Microbiol.*, 2021, **19**, 409.
12 C. A. A. van Boeckel and M. Petitou, *Angew. Chem., Int. Ed. Engl.*, 1993, **32**, 1671.